

# Sputter Process Optimization for $\text{Al}_{0.7}\text{Sc}_{0.3}\text{N}$ Piezoelectric Films

Valeriy Felmetsger  
PVD Process Development  
Department  
OEM Group, LLC  
Gilbert, Arizona, USA  
valeriy.felmetsger@oemgroupinc.com

Mikhail Mikhov  
PVD Process Development  
Department  
OEM Group, LLC  
Gilbert, Arizona, USA  
mikhailmikhov@oemgroupinc.com

Mehrdad Ramezani  
Electrical and Computer  
Engineering Department  
University of Florida  
Gainesville, Florida, USA  
mehram@ufl.edu

Roozbeh Tabrizian  
Electrical and Computer  
Engineering Department  
University of Florida  
Gainesville, Florida, USA  
rtabrizian@ece.ufl.edu

**Abstract**— $\text{Al}_{0.7}\text{Sc}_{0.3}\text{N}$  films were reactively sputtered from Al-Sc segmented targets by ac powered dual-cathode S-gun magnetron. 0.5-2.0  $\mu\text{m}$  thick films with homogeneous Sc concentration within 30 +/- 0.5 at. % across 200-mm wafers were grown at ambient temperature directly on Si (100) and on highly (110) textured Mo electrodes. Sputter process optimization, focused on improving film crystalline quality and reducing surface roughness, was performed using XRD, SEM, EDS, TEM, and AFM methods. In contrast to AlN films, which crystallinity typically improves with increasing film thickness due to growth of more thorough grains,  $\text{Al}_{0.7}\text{Sc}_{0.3}\text{N}$  texture degrades in thicker films. Technological solutions for smooth and highly c-axis oriented  $\text{Al}_{0.7}\text{Sc}_{0.3}\text{N}$  films were defined and tested. Introduction of AlN seed layer and deposition at low gas pressure remarkably suppressed growth of abnormal grains and improved crystallinity of the films. Highly c-axis oriented films with RC FWHM of  $1.6^\circ$  and surface roughness RMS of 2.3 nm were grown on Si as well as on Mo electrodes.

**Keywords**—AlScN film, Sc-doped AlN film, S-gun magnetron, reactive magnetron sputtering, crystal orientation

## I. INTRODUCTION

Piezoelectric wurtzite  $\text{Al}_{1-x}\text{Sc}_x\text{N}$  thin films ( $x < 0.43$ ) exhibit considerably higher electromechanical coupling coefficient  $k_{\text{eff}}^2$  compared to pure AlN films and therefore are very attractive for implementation in variety of electroacoustic devices. Recent progress in reactive magnetron sputtering of Sc-doped films enabled synthesizing high quality films suitable for mass production. Depending on  $x$  and sputter process capabilities, piezoelectric coefficient  $d_{33}$  can be increased up to 4-5.5 times with increasing atomic concentration of Sc [1, 2]. However due to material softening, increasing leakage current, and reducing Q-factor, only relatively low-doped films can be effectively used in FBAR type devices. Sc addition of 7-10 at. % enables increasing coupling coefficient while keeping elastic constants high enough. Post-deposition anneal in vacuum allows remarkably increasing  $k_{\text{eff}}^2$  in low Sc-doped films [3]. More challenging from sputter process view point films with high Sc content in the range of 20-40 at. % are extremely important for Piezo MEMS devices such as efficient energy harvesters requiring maximal coupling and ultra- and super-high frequency resonators for emerging 5G RF front-end systems requiring thin and ultrathin  $\text{Al}_{1-x}\text{Sc}_x\text{N}$  films with strong piezo-activity [4].

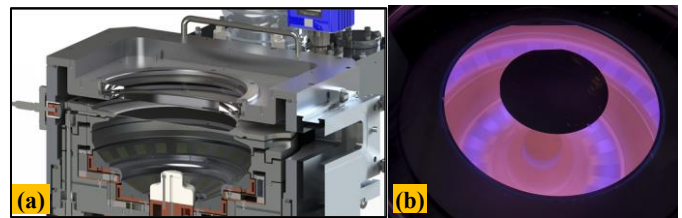


Fig. 1. Sputter technique for deposition of highly Sc-doped AlScN films: (a) S-gun cross-section and (b) magnetron discharge on segmented targets.

Performance of Piezo MEMS devices is substantially tied to  $\text{Al}_{1-x}\text{Sc}_x\text{N}$  sputter technology in terms of film crystallinity, texture, surface roughness, and intrinsic stress. Therefore, process optimization is pivotal to satisfy all these success criteria simultaneously.

Nowadays major process optimization challenges in deposition of highly Sc-doped  $\text{Al}_{1-x}\text{Sc}_x\text{N}$  films deal with preventing crystalline quality degradation [5], eliminating growth of abnormal cone-like grains [6-8], and effective managing of film stress. In this communication, we describe technological solutions for the reactive sputtering of smooth and highly oriented  $\text{Al}_{0.7}\text{Sc}_{0.3}\text{N}$  films. Sputter process optimization related to film crystallinity, texture, and surface roughness was performed using XRD, SEM, EDS, TEM, and AFM methods.

## II. EXPERIMENTAL DETAILS

### A. Sputter Technique for Growth of $\text{Al}_{0.7}\text{Sc}_{0.3}\text{N}$ Films

Endeavor-MX PVD cluster tool equipped with S-gun magnetrons was employed for the deposition of  $\text{Al}_{0.7}\text{Sc}_{0.3}\text{N}$  piezoelectric and Mo electrode thin films. The S-gun consists of two coaxially nested magnetrons equipped with ring-shape targets. In the magnetron for reactive sputtering, ac (40 kHz) power supply with floating output is connected directly between two targets thus enabling arc-free operation during deposition of dielectric films [9].

Depending on Sc content, 3 modifications of sputtering targets were employed: Al-Sc alloy containing 8 at. % Sc, Al targets with embedded Sc pellets enabling deposition of films with up to 14 at. % Sc [10], and segmented Al-Sc targets for the deposition of highly Sc-doped films.

New segmented target design combines alternated Al and Sc segments enabling uniform Sc distribution in  $Al_{1-x}Sc_xN$  films across the wafer. Advantage of this design is inexpensive fabrication process since it doesn't require employing complicated metallurgy as in a case of Al-Sc alloy targets. Moreover, variation of quantity and/or width of Al and Sc segments allows setting a certain composition of the film and controlling the composition radial homogeneity. Using this target set, 0.5-2.0  $\mu\text{m}$  thick  $Al_{0.7}Sc_{0.3}N$  films were grown directly on 200-mm Si (100) wafers and on Mo bottom electrodes deposited in the Endeavor cluster tool using dc powered S-gun. No external heat was applied to the wafer during deposition.

### B. Al-Sc Target Conditioning Prior to $Al_{1-x}Sc_xN$ Deposition

An important part of the S-gun AlN technology relates to the Al sputter targets preconditioning in Ar discharge for a few minutes prior to the deposition of AlN film on a product (device) wafer. The preconditioning, if repeated regularly before each product wafer deposition, enables keeping constant impedance of the S-gun and thus preserves excellent repeatability of film uniformity and stress from wafer to wafer. However we observed that sputtering of Al-Sc segmented targets in metallic mode during preconditioning led to synthesis of black color coating on some of the Al segments. Presumably this is  $Al_3Sc$ , polycrystalline brittle intermetallic compound having low density. Due to low Sc solid solubility in Al,  $Al_3Sc$  precipitations can appear in binary Al-Sc alloys after exposure to elevated temperature [10]. We assume that some of Al segments may receive higher temperature during sputtering which is sufficient for reaction with Sc atoms sputtered from the neighbor Sc segments on the surface of the Al segments.

The presence of  $Al_3Sc$  phase on the targets may have two negative effects on quality of  $Al_{1-x}Sc_xN$  films. The first one is film contamination by foreign particles which can be easily monitored at optical microscope. However other potential issue needs more detail investigation. If, besides of Al and Sc atoms, a flux of the species sputtered from the Al-Sc targets contains some  $Al_3Sc$  molecules, those molecules after interaction with nitrogen will be incorporated in stoichiometric  $Al_{1-x}Sc_xN$  film as clusters with different crystallinity and/or crystal orientation. To eliminate risk of film contamination with  $Al_3Sc$  precipitations, targets sputtering in poison mode for several minutes was added to the target preconditioning in metallic mode.

## III. RESULTS AND DISCUSSION

### A. Film Composition and Uniformity

To explore Sc distribution, energy dispersive x-ray spectroscopy (EDS) measurements were performed in 10 points across 200-mm Si wafer. EDS data showed that Sc content increased towards wafer edge from 28.5 to 30.5 at. % (Fig. 2), while Rutherford backscattering spectroscopy (RBS) completed in 5 points showed that composition of the film is highly uniform across the wafer and close to 30 +/- 0.5 at. %.

Typical film thickness map on 200-mm wafer presented in Fig. 3 shows uniformity 0.56% ( $1\sigma$ ).

### B. Surface Roughness

Remarkably higher surface roughness of highly Sc-doped films compared to AlN might be due to non-uniform nucleation,

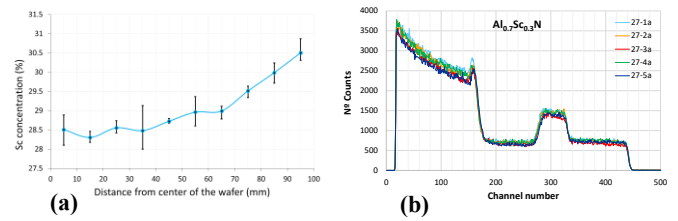


Fig. 2. Uniformity of Sc concentration in 720 nm AlScN film across 200-mm wafer: (a) EDS characterization results and (b) RBS data (RBS analyses completed at Madrid Polytechnic University by Prof. Marta Clement).

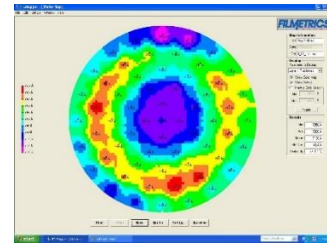


Fig. 3. Thickness map of  $Al_{0.7}Sc_{0.3}N$  film on 200-mm Si wafer measured by reflectometer in 61 points with edge exclusion 7 mm: 713.6 nm +/- 1.1%.

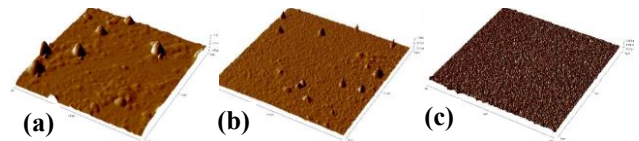


Fig. 4. AFM scans ( $10 \times 10 \mu\text{m}$ ) of 1  $\mu\text{m}$  thick  $Al_{0.7}Sc_{0.3}N$  films deposited (a) directly on Si wafer, (b) on Mo bottom electrode, and (c) on Si over AlN seed layer.

grain agglomeration, and appearance of faster growing abnormal cone-like grains which protrude from c-textured film [7, 8]. Those grains exhibit different from AlN (002) crystal orientation and thus reduce piezo activity of  $Al_{1-x}Sc_xN$  films. Since those grains are more resistive to wet and plasma etching, they can remarkably worsen quality of patterning processes. Hence important process optimization challenge is to find conditions reducing surface roughness and preventing growth of abnormal grains.

Experiments have shown that surface roughness was extremely dependable on the sputter process parameters and film thickness. 500 nm thick films were typically smooth and did not contain abnormal grains, while surface roughness gradually increased in thicker films. Therefore, to investigate influence of major sputter process parameters on film crystallinity and roughness, all further process optimization experiments were completed using relatively thick films. When 1  $\mu\text{m}$  thick  $Al_{0.7}Sc_{0.3}N$  films were deposited on Si or on Mo using regular for AlN sputter recipes, these abnormal grains could be clearly seen on AFM scans (Fig. 4a, 4b).

### C. Influence of Sputter Gases and Wafer Temperature

Ar and  $N_2$  gas flows varied in wide range to explore influence on film crystallinity, orientation, and surface morphology. It was found that higher ac sputter power and lower gas pressure (lowering both Ar and  $N_2$  gas flows) in a sputter recipe were beneficial for growth of smooth films. However, films deposited with high  $N_2$  exhibited remarkably better crystal

orientation. Wafer temperature was critical parameter and excessively high temperature ( $> 400\text{ }^{\circ}\text{C}$ ) led to growth of films with abnormally rough surface. Therefore all films were grown at ambient temperature. In this case wafer temperature raised up to about  $350\text{ }^{\circ}\text{C}$  during deposition due to energy of condensation and interaction with S-gun magnetron discharge. Energetic species bombardment from ac magnetron plasma enabled deposition of highly c-axis oriented  $\text{Al}_{0.7}\text{Sc}_{0.3}\text{N}$  without external heating and/or biasing.

We explored a few methods to suppress growth of the abnormal grains and found that AlN seed layer might be very efficient solution to reduce surface roughness as well as to improve film crystalline quality.

#### D. Influence of AlN Seed Layer on $\text{Al}_{0.7}\text{Sc}_{0.3}\text{N}$ Film Crystallinity and Surface Roughness

Increasing Sc content above about 20% leads to deterioration of crystalline quality of  $\text{Al}_{1-x}\text{Sc}_x\text{N}$  films exhibiting wider x-ray rocking curves and/or appearance of phases with different from c-axis crystal orientation. Hence the first priority challenge is to find sputter conditions ensuring development of strong single c-axis orientation in films.

One of the most effective technological approaches to create well-oriented metal electrodes for electro-acoustic devices is based on the application of “seed layers” such as Ti and AlN, modifying surface morphology and stimulating formation of well-oriented grains due to decreasing the crystallization energy of the metal film through mechanism of the coherent heteroepitaxial nucleation [12]. Therefore depositing AlN underlayer prior to  $\text{Al}_{1-x}\text{Sc}_x\text{N}$  sputtering is reasonable approach. It was confirmed for low Sc-doped films [13]: an addition of 100 nm thick AlN seed layer promoted growth of better (0001)-textured  $\text{Al}_{0.84}\text{Sc}_{0.16}\text{N}$  films even when there was vacuum break after AlN deposition.

We found that deposition of a thin (50 nm) AlN seed layer without vacuum break in cluster sputter tool right before  $\text{Al}_{0.7}\text{Sc}_{0.3}\text{N}$  sputtering promotes more uniform nucleation and thus remarkably reduces roughness of the  $\text{Al}_{0.7}\text{Sc}_{0.3}\text{N}$  films deposited on Si as well as on Mo bottom electrode. Surface roughness RMS of the films deposited over the AlN seed layer reduced to 2.3 - 3.5 nm, no abnormal grains were observed in this case (Fig. 4c).

#### IV. OPTIMIZED $\text{Al}_{0.7}\text{Sc}_{0.3}\text{N}$ SPUTTER PROCESS

Besides introduction of the seed layer, relatively low sputter pressure during  $\text{Al}_{0.7}\text{Sc}_{0.3}\text{N}$  sputtering was found beneficial for growth of highly oriented and smooth films. Films deposited with the lowest Ar gas flow (1.5 sccm still sustains stable ac discharge in the S-gun) exhibited the lowest surface roughness when  $\text{N}_2$  flow was sufficient to preserve operation of the magnetron in poison mode. With the same low Ar flow, appearance of the films depended to sputter power. Variation of ac power from 2 kW to 5 kW showed that the lower the ac power, the higher the surface roughness. Therefore, basic sputter recipe was established with ac of 5 kW and Ar of 1.5 sccm.

Optimization of  $\text{N}_2$  flow was not as straightforward as optimization of Ar flow. Deposition with low Ar and low  $\text{N}_2$  flows enabled smoother films, while using relatively high  $\text{N}_2$

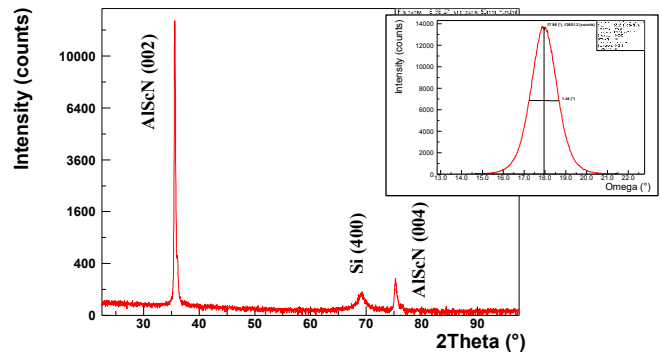


Fig. 5. X-ray  $\theta$ - $2\theta$  scan of 720 nm thick  $\text{Al}_{0.7}\text{Sc}_{0.3}\text{N}$  film on Si (100) wafer. Inset is x-ray rocking curve around AlScN (002) peak [FWHM =  $1.44^{\circ}$ ].

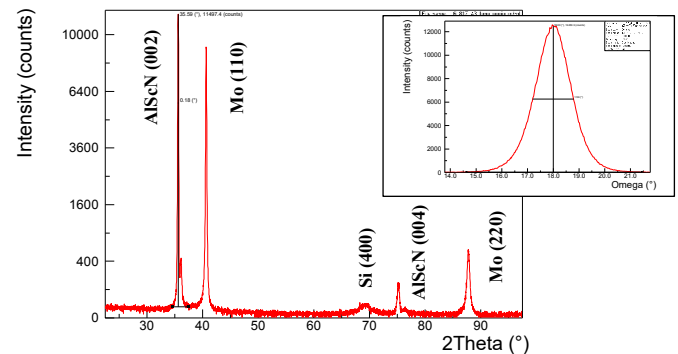


Fig. 6. X-ray  $\theta$ - $2\theta$  scan of 1  $\mu\text{m}$  thick  $\text{Al}_{0.7}\text{Sc}_{0.3}\text{N}$  film on Mo electrode. Inset is rocking curve around AlScN (002) peak [FWHM =  $1.58^{\circ}$ ].

flow of 20 sccm (optimal  $\text{N}_2$  flows for AlN films are in the range of 15-17 sccm when ac power is 5 kW) was found beneficial for film crystal orientation but aggravated film roughness. Previously published data showed that with increasing  $\text{N}_2$  concentration in plasma the density of the abnormal grains decreased and deposition in 100%  $\text{N}_2$  atmosphere enabled very smooth surface with the lowest density of misoriented grains [6].

We found that deposition by the S-gun with higher  $\text{N}_2$  enabled better  $\text{Al}_{0.7}\text{Sc}_{0.3}\text{N}$  nucleation and improved crystal orientation. But film surface roughness increased in case of deposition of thicker films (1 - 2  $\mu\text{m}$ ) with high  $\text{N}_2$  pressure. To satisfy both requirements (strong c-axis orientation and smooth surface), we split sputter recipe in two steps. In the first step, relatively high  $\text{N}_2$  flow of 20 sccm was employed during deposition of 20-30% of film thickness to ensure nucleation and growth of highly oriented film. Then in the second step, remaining 70-80% of film thickness was deposited with  $\text{N}_2$  flow reduced to 15 sccm to ensure growth of smooth film.

Using AlN seed layer and optimization of Ar and  $\text{N}_2$  flows allowed depositing highly c-axis oriented films on Si. Presence of both AlScN (002) at  $2\theta = 35.6^{\circ}$  and AlScN (004) at  $2\theta = 75.27^{\circ}$  reflections indicates that film exhibits strong single crystal orientation with rocking curve FWHM =  $1.44^{\circ}$  (Fig. 5).

X-ray  $\theta$ - $2\theta$  scan of 1  $\mu\text{m}$  thick  $\text{Al}_{0.7}\text{Sc}_{0.3}\text{N}$  film deposited on 100 nm thick highly (110) oriented Mo bottom electrode showed similar pattern and strong single crystal orientation as observed on Si with rocking curve FWHM =  $1.58^{\circ}$  (Fig. 6).



High-resolution XTEM images and corresponding fast Fourier transforms show columnar microstructure with strong texture (Fig. 7). However it is well seen that  $\text{Al}_{0.7}\text{Sc}_{0.3}\text{N}$  is worse textured than  $\text{AlN}$  seed layer. FFT analyses performed through the film thickness elicited that  $\text{Al}_{0.7}\text{Sc}_{0.3}\text{N}$  texture deteriorates towards the film surface (Fig. 8).

Our data show also that in contrast to  $\text{AlN}$  films, which crystallinity typically improves with increasing film thickness due to growth of more thorough grains, texture of  $\text{Al}_{0.7}\text{Sc}_{0.3}\text{N}$  films degrades in thicker films.

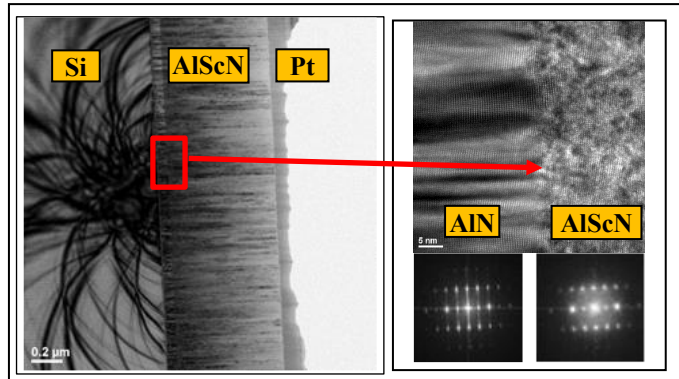


Fig. 7. High-resolution XTEM images and corresponding fast Fourier transforms.

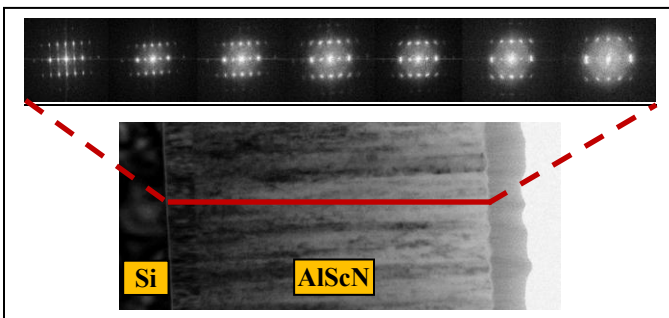


Fig. 8. Fast Fourier transforms of high-resolution XTEM extracted from TEM images taken through the  $\text{Al}_{0.7}\text{Sc}_{0.3}\text{N}$  film thickness.

## V. CONCLUSION

$\text{Al}_{1-x}\text{Sc}_x\text{N}$  films with Sc content of 20-40 at. % are important for variety of Piezo MEMS devices requiring maximal coupling. Challenges in development of sputter processes for these films deal with reliable control of film crystalline quality, uniformity, surface roughness, and stress. Reactive sputtering by ac powered S-gun magnetron equipped with Al-Sc segmented targets enabled deposition of  $\text{Al}_{0.7}\text{Sc}_{0.3}\text{N}$  films with homogeneous Sc concentration within 30 +/- 0.5 at. % and thickness deviation around +/-1.0% across 200-mm wafers. Technological solutions for the reactive sputtering of smooth and highly c-axis oriented  $\text{Al}_{0.7}\text{Sc}_{0.3}\text{N}$  films were defined and tested. Introduction of  $\text{AlN}$  seed layer and deposition at low gas pressure enabled growth of highly c-axis oriented 1  $\mu\text{m}$  thick films exhibiting RC FWHM = 1.6° on Si as well as on Mo electrode and low surface roughness with RMS = 2.3 nm.  $\text{Al}_{0.7}\text{Sc}_{0.3}\text{N}$  films exhibit columnar microstructure with strong texture but it was found that texture deteriorates towards film surface and crystalline quality degradation increases with film thickness. More detail

exploration is required to overcome these issues and further optimize sputter processes for highly Sc-doped films.

## REFERENCES

- [1] M. Akiyama, K. Kano, and A. Teshigahara, "Influence of growth temperature and scandium concentration on piezoelectric response of scandium aluminum nitride alloy thin films" *Appl. Phys. Lett.* 95 (2009) 162107.
- [2] Y. Lu, M. Reusch, N. Kurz, A. Ding, T. Christoph, M. Prescher, L. Kirste, O. Ambacher, and A. Zukauskaitė, "Elastic modulus and coefficient of thermal expansion of piezoelectric  $\text{Al}_{1-x}\text{Sc}_x\text{N}$  (up to  $x = 0.41$ ) thin films," *Appl. Materials* 6 (7), 076105 (2018).
- [3] M. Clement, V. Felmetsger, T. Mirea, J. Olivares, and E. Iborra, "Effects of post-deposition vacuum annealing on the piezoelectric properties of  $\text{AlScN}$  thin films sputtered on 200 mm production wafers," *Proceedings of the IEEE Int. Ultrasonics Symp.*, Kobe, Japan, October 22-25, 2018.
- [4] S. Mahon, "The 5G Effect on RF Filter Technologies", *IEEE Trans. Semicon. Manufac.* 30 (2017) 494-499.
- [5] A. Zukauskaitė, G. Wingqvist, J. Palisaitis, J. Jensen, P. O. A. Persson, R. Matloub, P. Murali, Y. Kim, J. Birch, and L. Hultman, "Microstructure and dielectric properties of piezoelectric magnetron sputtered w- $\text{Sc}_x\text{Al}_{1-x}\text{N}$  thin films," *J. Appl. Phys.* 111 (2012) 093527.
- [6] Y. Lu, M. Reusch, N. Kurz, A. Ding, T. Christoph, L. Kirste, V. Lebedev, and A. Zukauskaitė, "Surface morphology and microstructure of pulsed dc magnetron sputtered piezoelectric  $\text{AlN}$  and  $\text{AlScN}$  thin films," *Phys. Status Solidi A* (2017) 1700559.
- [7] S. Fichtner, N. Wolff, G. Krishnamurthy, A. Petraru, S. Bohse, F. Lofink, S. Chemnitz, H. Kohlstedt, L. Kienle, and B. Wagner, "Identifying and overcoming the interface originating c-axis instability in highly Sc enhanced  $\text{AlN}$  for piezoelectric micro-electromechanical systems", *J. Appl. Phys.*, 122 (2017) 35301.
- [8] C. S. Sandu, F. Parsapour, S. Mertin, V. Pashchenko, R. Matloub, T. LaGrange, B. Heinz, and P. Murali "Abnormal grain growth in  $\text{AlScN}$  thin films induced by complexion formation at crystallite interfaces," *Phys. Status Solidi A* (2018) 1800569.
- [9] V. Felmetsger, P. Laptev, and S. Tanner, "Design, operation mode, and stress control capability of S-gun magnetron for ac reactive sputtering," *Surf. Coat. Technol.* 204 (2009) 840-844.
- [10] G. Novotny and A. Ardell, "Precipitation of  $\text{Al}_3\text{Sc}$  in binary Al-Sc alloys," *Materials Science and Engineering A318* (2001) 144-154.
- [11] V. Felmetsger, P. Laptev, and S. Tanner, "Crystal orientation and stress in ac reactively sputtered  $\text{AlN}$  films on Mo electrodes for electro-acoustic devices", 2008 *IEEE Int. Ultrasonics Symp.*, Beijing, 2008, pp. 2146-2149.
- [12] T. Kamohara, M. Akiyama, N. Ueno, K. Nonaka, and N. Kuwano, "Local epitaxial growth of aluminum nitride and molybdenum thin films in fiber texture using aluminum nitride interlayer", *Appl. Phys. Lett.*, 89 (2006), 071919.
- [13] F. Parsapour, V. Pashchenko, S. Mertin, C. Sandu, N. Kurz, P. Nicolay, and P. Murali "Ex-situ  $\text{AlN}$  seed layer for (0001)-textured  $\text{Al}_{0.84}\text{Sc}_{0.16}\text{N}$  thin films grown on  $\text{SiO}_2$  substrates," 2017 *IEEE Int. Ultrasonics Symp.*, Bellingham, Washington, 2017.